Proc. Natl. Acad. Sci. USA
Vol. 89, pp. 2654–2658, April 1992
Biochemistry

DNA helical stability accounts for mutational defects in a yeast replication origin

(DNA replication/autonomously replicating sequences/DNA unwinding element/energetics)

DARREN A. NATALE, ANN E. SCHUBERT, AND DAVID KOWALSKI*

Molecular and Cellular Biology Department, Roswell Park Cancer Institute, Buffalo, NY 14263

Communicated by Martin Gellert, December 20, 1991

ABSTRACT **Earlier studies on the H4 autonomously replicating sequence (*ARS*) identified a DNA unwinding element (DUE), a required sequence that is hypersensitive to single-strand-specific nucleases and serves to facilitate origin unwinding. Here we demonstrate that a DUE can be identified in the C2G1 *ARS*, a chromosomal replication origin, by using a computer program that calculates DNA helical stability from the base sequence. The helical stability minima correctly predict the location and hierarchy of the nuclease-hypersensitive sites in a C2G1 *ARS* plasmid. Nucleotide-level mapping shows that the nuclease-hypersensitive site at the *ARS* spans a 100-base-pair sequence in the required 3′-flanking region. Mutations that stabilize the DNA helix in the broad 3′-flanking region reduce or abolish *ARS*-mediated plasmid replication, indicating that helical instability is required for origin function. The level of helical instability is quantitatively related to the replication efficiency of the *ARS* mutants. Multiple copies of either a consensus-related sequence present in the C2G1 *ARS* or the consensus sequence itself in synthetic *ARS* elements contribute to DNA helical instability. Our findings indicate that a DUE is a conserved component of the C2G1 *ARS* and is a major determinant of replication origin activity.**

Origins of DNA replication in *Saccharomyces cerevisiae* (1–4) were originally identified as cis-acting sequences that promote autonomous replication of plasmids (5). A comparison of such autonomously replicating sequences (*ARS*s) revealed an 11-base-pair (bp) core consensus element: WTTTATRTTTW (W is A or T and R is A or G) (6). The core consensus element is necessary but not sufficient for origin function. Deletion analyses have revealed that efficient replication requires a broad 3′-flanking region that spans on the order of 100 bp (7–10); however, the minimum length is difficult to define since the contiguous vector sequence can strongly influence *ARS* function (reviewed in ref. 11). Unlike the consensus element, the required 3′-flanking region exhibits little DNA sequence similarity among *ARS* elements. However, the required 3′-flanking region contains multiple near matches (9 or 10 of 11 bp) to the core consensus sequence (9) that vary in number, spacing, and orientation among *ARS* elements.

The required 3′-flanking region of the H4 *ARS* and the 2-μm plasmid *ARS* is hypersensitive to single-strand-specific nucleases in negatively supercoiled DNA (12, 13). Nuclease hypersensitivity of H4 *ARS* derivatives with deletions in the 3′-flanking region correlates with the ability of the derivatives to transform yeast at high frequency (12). The hypersensitive site identifies the plasmid DNA sequence with the lowest free energy cost for unwinding (14). The ease of unwinding the H4 *ARS* nuclease-hypersensitive element is biologically relevant since mutations in the 3′-flanking region that raise the free energy cost for unwinding—and compromise replication efficiency—can be suppressed in yeast cells at elevated growth temperature (15). We call the nuclease-hypersensitive sequence a DNA unwinding element (DUE) and have proposed that, like the DUE in the *Escherichia coli* chromosomal origin (16, 17), the DUE in yeast origins facilitates the initial unwinding of parental strands, permitting the entry of replication enzymes into the DNA helix (15).

A DUE may be a conserved component of DNA replication origins in cells of bacteria, yeast, and mammals (15–22). To facilitate further characterization of replication origins, it would be useful to be able to identify DUEs from DNA sequence information and to quantify their ease of unwinding. DUEs often occur in A+T-rich sequences; however, the A+T content of DUEs does not predict hypersensitivity to single-strand-specific nucleases (13) or replication origin function (16). Nuclease hypersensitivity likely reflects DNA helical instability (14, 16), which is largely determined by stacking interactions between nearest-neighbor bases and, therefore, depends on the DNA sequence (23–25).

In this paper, we describe an approach that uses DNA sequence information to identify potential DUEs and examine the involvement of the DUE in replication origin function. The approach is based on the fact that the helical stability of a DNA oligomer sequence can be reliably calculated from the known thermodynamic properties of the component nearest-neighbor dinucleotides (25). Here, we test the applicability of helical stability calculations to identify the nuclease hypersensitive sites in a plasmid containing a yeast replication origin. Furthermore, we examine the relationship between helical stability and replication efficiency of mutant derivatives of the replication origin to quantitatively assess the involvement of a DUE. We chose to examine the C2G1 *ARS* because quantitative replication efficiencies have been determined for a large collection of derivatives bearing mutations in the broad 3′-flanking region (9) and because, unlike certain *ARS* elements (3), it is a chromosomal replication origin [also called *ARS307* (26)].

MATERIALS AND METHODS

Enzymes. Enzymes were from commercial suppliers as follows: mung bean nuclease, Pharmacia; restriction endonucleases, New England Biolabs; bacterial alkaline phosphatase, Worthington; polynucleotide kinase, United States Biochemical.

DNA. pC2G1 (a gift from Carol Newlon, UMDNJ–New Jersey Medical School) is a YIp5 derivative containing the 522-bp *Eco*RI/*Cla* I C2G1 *ARS* fragment (27) of known sequence (9, 26). The short *Eco*RI/*Cla* I fragment of YIp5 is present twice in the following arrangement: *Eco*RI–*Cla* I–(C2G1)–*Eco*RI–*Cla* I.

The publication costs of this article were defrayed in part by page charge payment. This article must therefore be hereby marked "*advertisement*" in accordance with 18 U.S.C. §1734 solely to indicate this fact.

Abbreviation: DUE, DNA unwinding element.

*To whom reprint requests should be addressed.

E. coli HB101 containing pC2G1 was grown in Luria–Bertani broth. Cells were lysed by boiling in the presence of lysozyme (28) and plasmid DNA was purified by two rounds of CsCl gradient centrifugation (29). The superhelical density of plasmids prepared by this method is -0.065 ± 0.002 as determined by two-dimensional agarose gel electrophoresis of plasmid topoisomers (14).

Single-Strand-Specific Nuclease Reactions. Supercoiled pC2G1 (10 μg) was preincubated at 37°C in 100 μl of 10 mM Tris·HCl, pH 7.0/1 mM Na_2EDTA. After addition of mung bean nuclease (39 units in 10 μl; units are defined by Pharmacia), the reaction proceeded for 30 min. Reactions were quenched (13), and the DNA was purified by phenol extraction and ethanol precipitation. Under these conditions, the nuclease introduces a single nick per molecule, since the initial nick converts the supercoiled plasmid to a nuclease-resistant relaxed form (30).

Global and Nucleotide Level Mapping of Mung Bean Nuclease Nicks. Supercoiled pC2G1 was singly nicked by mung bean nuclease as described above. The sites of nuclease hypersensitivity were determined as described by a method that directly maps nuclease nicks (12, 14, 16).

The positions of nuclease nicks were determined at nucleotide resolution by electrophoresis of purified single-end-labeled DNA fragments containing nicks on denaturing polyacrylamide gels alongside Maxam and Gilbert sequencing ladders (31) of unnicked fragments as described (32). The sequenced fragment extends from a labeled *Eco*RI site [position 2 of the published sequence (9)] to an *Alu* I site (position 282) for the consensus A-rich strand (see Fig. 2) and from a labeled *Ase* I site (position 326) to a *Cla* I site (within the vector beyond an *Eco*RI site) for the consensus T-rich strand.

Computer Analyses. A computer program was developed to calculate the free energy difference (ΔG) between the duplex and single-stranded states for multiple overlapping segments, or "windows," of DNA sequence. The ΔG was calculated from the values for $\Delta H°$ and $\Delta S°$ using equation 14 of ref. 33 and a calculated t_m, which was adjusted to reflect the difference in salt concentration between our nuclease hypersensitivity assay conditions and those used for the determination of thermodynamic data (25) used by the program.

To specifically determine the helical stability of the 3′-flanking region of C2G1 *ARS* deletion derivatives, we calculated the free energy required to strand-separate the 100-bp segment of DNA 3′ to the core consensus. The position of the 100-bp window was permitted to vary up to 10 bp to allow for uncertainty in the precise location of DNA unwinding. The helical stability of the 3′-flanking region was taken as the lowest ΔG value obtained. Subsequent analysis revealed that correlations quantitatively similar to those reported are also obtained when no variation in window position is permitted (data not shown).

RESULTS

Nuclease-Hypersensitive Sites in a C2G1 *ARS* Plasmid. We mapped the nicks made by the single-strand-specific nuclease in pC2G1 relative to unique restriction sites by electrophoretic analysis of the denatured DNA products. The procedure generates three bands for each specific nuclease-hypersensitive site: a pair of bands derived from DNA strands whose lengths correspond to the distance from a unique ^{32}P-labeled restriction site to mung bean nuclease nicks in either the top or bottom strand and a unit length band derived from the strand that is not nicked. Two different restriction endonucleases (*Nco* I, *Ava* I) were used to unambiguously map the sites (Fig. 1). Asterisks mark the band pair in each lane that corresponds to nuclease recognition of the C2G1 *ARS*. The intensity of this band pair relative to the other band pair identifies the C2G1 *ARS* as the most nuclease-hypersensitive region in the plasmid. The minor band pair in each lane corresponds to a previously characterized site in the vector at the terminator region of the ampicillin-resistance gene (14).

Sequence-Level Analysis of Mung Bean Nuclease Nicks at the C2G1 *ARS*. We determined the precise sequence that was hypersensitive to mung bean nuclease in the C2G1 *ARS* (Fig. 2). Both DNA strands, the consensus A-rich strand (*Left*) and the consensus T-rich strand (*Right*), were examined. Mung bean nuclease (nuclease lanes) selectively recognizes an ≈100-bp region of the DNA in both strands (indicated by the bracketed bands). The region recognized is similar for each strand (compare bracketed region with nucleotide numbering). The results show that the nuclease-hypersensitive region is located primarily within the ≈100 bp 3′ to the T-rich strand of the consensus element (boxed).

Quantitative Analysis of the DNA Helical Stability of pC2G1. We developed a computer program that uses the thermodynamic data for nearest-neighbor dinucleotides (25) to calculate the free energy difference between the duplex and single-stranded states for a given window, which slides along the DNA sequence. This free energy difference (ΔG) is a quantitative measure of DNA helical stability. Our nuclease-hypersensitivity assay empirically determines the most-easily unwound region(s) in a plasmid molecule (14). We therefore sought to test the correspondence between the pC2G1 site(s) recognized by the nuclease and the site(s) calculated to have the lowest free energy requirement for DNA strand separation. We used a 100-bp window size since that is the approximate length of the region recognized by the single-strand-specific nuclease.

A helical stability (ΔG) plot for pC2G1 (Fig. 3) shows a minimum (dashed line) between positions 400 and 500, indicating that this region is predicted to be the most-easily unwound in the plasmid. The major nuclease-hypersensitive site, at the C2G1 *ARS* (Fig. 3, heavy arrow), colocalizes with the predicted helical-stability minimum. The minor nuclease-hypersensitive site, at the terminator region of the ampicillin-resistance gene (Fig. 3, thin arrow), occurs at the second-lowest ΔG minimum. Thus, the computer program correctly

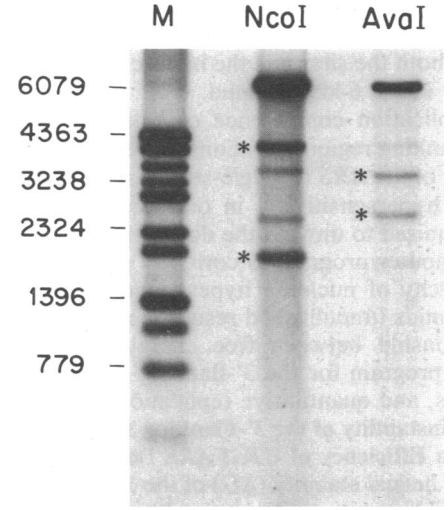

FIG. 1. Global mapping of mung bean nuclease-hypersensitive sites in pC2G1. Mung bean nuclease-treated pC2G1 was cut and 5′ ^{32}P-end-labeled at a single restriction endonuclease site before irreversible denaturation with glyoxal and agarose gel electrophoresis. Selected marker (lane M) sizes (in nucleotides) are indicated on the left. The bands that result from mapping with two different restriction endonucleases (*Nco* I, *Ava* I) are shown. Asterisks mark the band pair in each lane that results from nicking in the C2G1 *ARS* region (see text). The intense band at 6079 bases (pC2G1 unit length) is derived from the strand that remains intact after each molecule is singly nicked by mung bean nuclease.

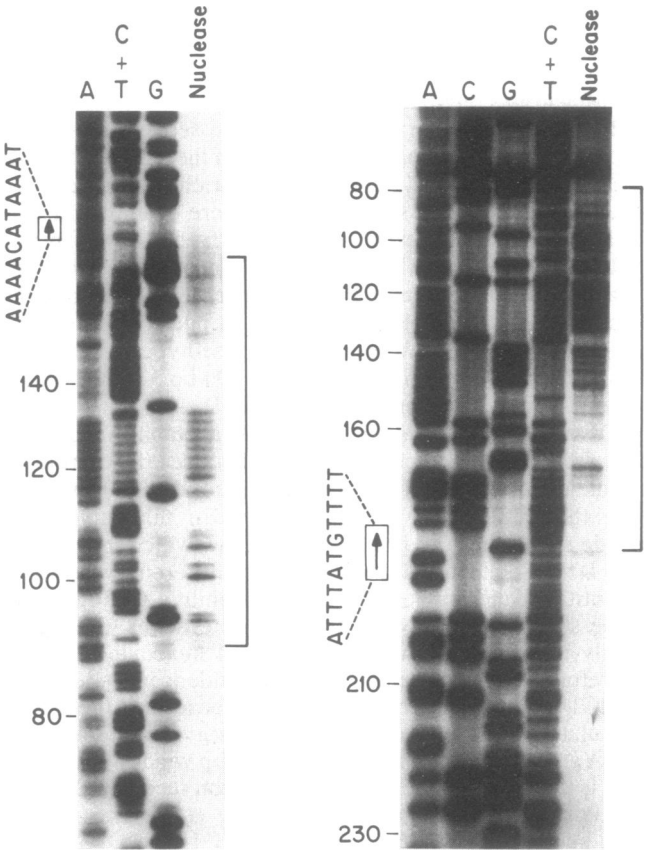

FIG. 2. Nucleotide-level mapping of mung bean nuclease nicks at the C2G1 *ARS*. Mung bean nuclease-nicked DNA (nuclease lanes) was separated by electrophoresis alongside Maxam and Gilbert sequencing lanes. The consensus element A-rich strand (*Left*) and T-rich strand (*Right*) are indicated by boxes. Arrows within the boxes indicate the 5′ → 3′ polarity of the DNA strand. Brackets indicate the sequence containing nuclease-specific nicks. The intense band in the nuclease lane (*Right*) that is not included in the bracket is an artifact of DNA renaturation (32). Nucleotide numbering is according to Palzkill and Newlon (9).

predicted both the sites and the hierarchy of nuclease hypersensitivity in the 6-kbp plasmid.

The replication competence of plasmids containing H4 *ARS* 3′-flanking region mutations correlates with the hypersensitivity of the *ARS* to single-strand-specific nuclease (12). Nuclease hypersensitivity, in our assay, reflects the free energy required to unwind the double helix (14). The ability of the computer program to correctly predict both the sites and hierarchy of nuclease hypersensitivity for pC2G1 and other plasmids (unpublished results) prompted us to look at the relationship between free energy, calculated by the computer program for the 3′-flanking region of C2G1 *ARS* derivatives, and quantitative replication efficiency.

Helical Instability of the 3′-Flanking Sequence Parallels the Replication Efficiency of C2G1 *ARS* Deletion Derivatives. In Fig. 4, the helical stability (ΔG) of the 3′-flanking region and the plasmid loss rate as determined by Palzkill and Newlon (9) are plotted according to size of deletion of yeast DNA for a series of external deletion mutants. The figure shows that the free energy cost for unwinding the 3′-flanking region of deletions that extend up to position 91 remains virtually constant and then increases dramatically with increasing deletion size. The dramatic increase in the free energy cost for unwinding exhibited by the larger deletions indicates that the vector DNA brought into the required 3′-flanking region is more difficult to unwind than the yeast DNA it replaces. The plasmid loss rate also exhibits a virtual constancy for the

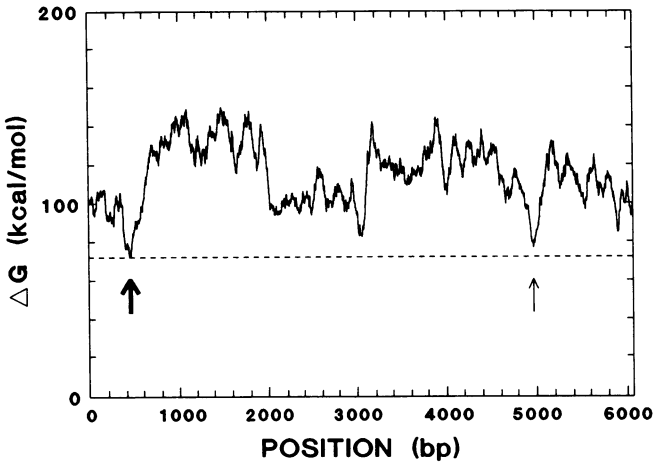

FIG. 3. Computer-calculated DNA helical stability for pC2G1. DNA helical stability (ΔG) was calculated as described in *Materials and Methods* and is plotted versus position. Dashed line is drawn at the free energy minimum for the plasmid that occurs between positions 400 and 500. The location of the nuclease-hypersensitive site at the C2G1 *ARS* is indicated by the heavy arrow, and the location of the nuclease-hypersensitive site within the vector is indicated by the thin arrow.

smaller deletions (allowing for error) before it increases markedly for deletions beyond position 91. The free energy cost for unwinding C2G1 *ARS* derivatives with progressive deletions into the 3′-flanking region closely parallels plasmid loss rate both by inspection (Fig. 4) and by linear regression analysis (correlation coefficient, 0.96). Plasmid loss rate represents the fraction of yeast cells that lose plasmid per generation during growth in nonselective liquid medium. As such, a lower plasmid loss rate is indicative of more efficient replication. The deletion derivatives that replicate more efficiently have a lower free energy cost for unwinding—i.e., greater helical *instability*—than those that replicate inefficiently. Therefore, the results in Fig. 4 indicate a quantitative relationship between helical instability and replication origin efficiency.

The C2G1 *ARS* derivative with the greatest free energy requirement that still gives high-frequency transformation is external deletion 133, with a free energy of strand separation of 112.4 kcal/mol (1 cal = 4.184 J) (calculated for the conditions described in *Materials and Methods*). Deletion of

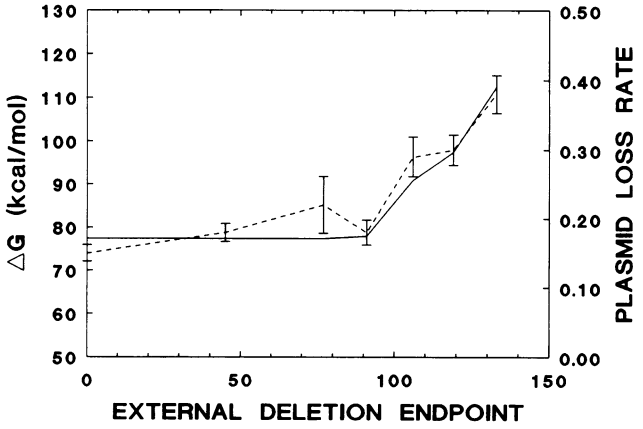

FIG. 4. Helical stability of the C2G1 *ARS* 3′-flanking region for a series of external-deletion derivatives. Helical stability of the 3′-flanking region (ΔG, solid line) and the plasmid loss rate (dashed line) are plotted according to the deletion end point for each *ARS* derivative. Error bars indicate standard error for the plasmid loss rates determined by Palzkill and Newlon (9).

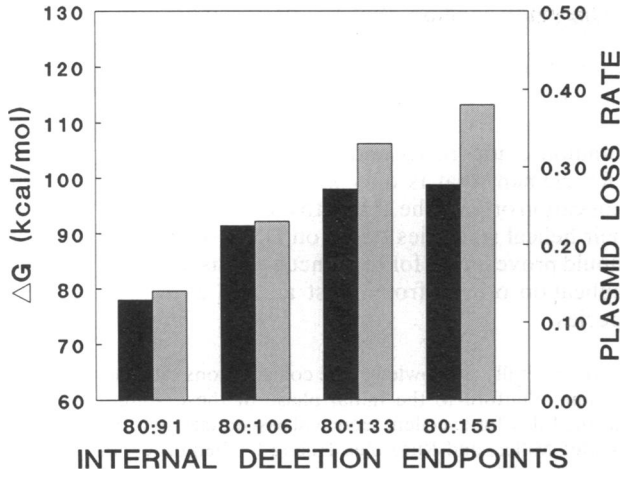

FIG. 5. Helical stability of the C2G1 *ARS* 3′-flanking region for a series of internal-deletion derivatives. Helical stability of the 3′-flanking region (ΔG, solid bars) and plasmid loss rate (shaded bars) for various internal-deletion derivatives are plotted on a histogram. Each of the derivatives shown shares a common end point. Plasmids in the internal-deletion series are named according to the deletion end points (L:R), where L is the left (consensus distal) end point and R is the right (consensus proximal) end point.

an additional 22 bp (external deletion 155) leads to loss of high-frequency transformation (9) and an increase in the ΔG to 115.9 kcal/mol. Thus, a threshold free energy value for the C2G1 *ARS* may exist between 112.4 and 115.9 kcal/mol, above which replication cannot be initiated.

In Fig. 5, the helical stability (ΔG) and plasmid loss rate for a series of internal deletion derivatives that share a common end point are plotted on a histogram. The size of each internal deletion increases toward the consensus from left (derivative 80:91) to right (derivative 80:155). A comparison across the series reveals that the changes in helical stability correlate with changes in plasmid loss rate (correlation coefficient, 0.96), consistent with the correlation noted for the external deletion derivatives. In addition, the ΔG values for these functional internal deletion derivatives all fall below the threshold ΔG value estimated for the nonfunctional external deletion derivative.

Comparison of the ΔG values for external and internal deletion derivatives that share a common deletion end point reveals the effect of bringing different sequences into the same 3′-flanking position. External deletion 155 and internal deletion derivative 80:155 remove an equal amount of the nuclease-hypersensitive sequence (Fig. 2, positions 81–154). However, as a result of the new sequences brought into the 3′-flanking region, the free energy required to strand-separate the functional 80:155 derivative (98.8 kcal/mol) is much less than that required for the nonfunctional external deletion derivative (115.9 kcal/mol). The difference in *ARS* function cannot be accounted for by a difference in the number of near matches to the consensus (9) since a computer-aided search reveals that neither deletion derivative contains a 9 of 11 or better match within the 3′-flanking region (up to 460 bp from the consensus).

Multiple Copies of an *ARS* Consensus Contribute to Helical Instability. Palzkill and Newlon (9) showed that the number of tandem copies of a synthetic fragment containing a perfect match to the C2G1 *ARS* core consensus element roughly correlated with plasmid replication efficiency. The 26-bp synthetic fragment consisted of the consensus element embedded in a sequence designed to confer overall a reduced A+T content (62%) relative to that of natural *ARS* elements [≥73% (6)]. The unwinding ability of these synthetic *ARS* elements was not determined.

Helical stability plots for plasmid constructs bearing one, two, or four synthetic fragments containing perfect matches to the consensus are shown in Fig. 6. Arrows denote perfect matches to the consensus, and the number of arrows indicates the number of tandemly repeated 26-bp synthetic fragments in each synthetic *ARS* element. The results show that despite the relatively low A+T content of the synthetic fragments (held constant across the series), an increasing number of perfect matches to the consensus results in a decreasing free energy cost for unwinding—i.e., increasing helical instability. The increase in helical instability is accompanied by an increase in replication efficiency—from no high-frequency transformation for the synthetic *ARS* bearing one copy of the fragment to a decrease in the plasmid loss rates of synthetic *ARS* elements bearing two (loss rate, 0.31) or four (loss rate, 0.26) synthetic consensus fragments. Other artificial *ARS* constructs (9) exhibit a similar relationship between helical instability and replication efficiency (data not shown).

DISCUSSION

We have identified a DNA sequence element that facilitates localized unwinding at the C2G1 *ARS*. The easily unwound sequence corresponds to the 100-bp region that is hypersensitive to single-strand-specific nuclease in negatively supercoiled DNA (Fig. 2). Mutational analysis has shown that the same broad region of the C2G1 *ARS* is required for plasmid replication in yeast (9). Our studies reveal that the nuclease hypersensitive element in the C2G1 *ARS*, like those in the H4 *ARS* (12) and 2-μm plasmid *ARS* (13), resides primarily in the required sequence 3′ to the consensus T-rich strand.

Single-strand-specific nuclease hypersensitivity in our assay reflects a low free energy requirement for localized DNA unwinding (14). Here we introduce the use of a computer program that makes use of experimentally determined thermodynamic parameters of the DNA sequence (25) to calculate the free energy difference between the duplex and single-stranded states—i.e., DNA helical stability. Calcula-

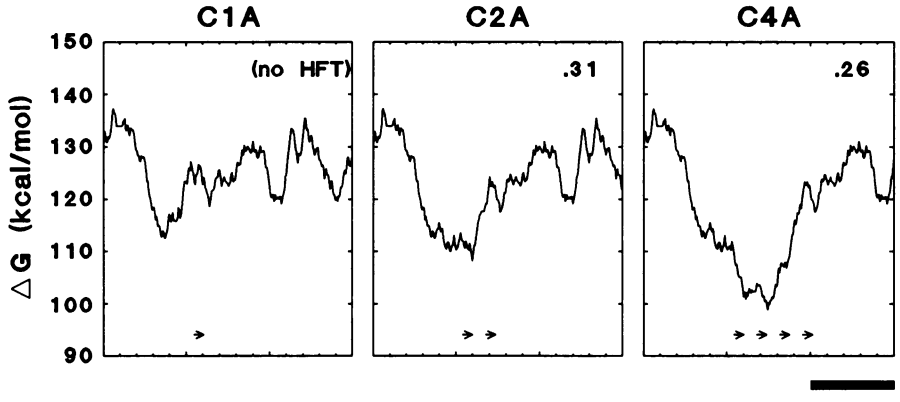

FIG. 6. Helical stability of synthetic *ARS* elements containing multiple copies of the C2G1 *ARS* core consensus sequence. Helical stability plots for plasmid constructs C1A, C2A, and C4A (9) bearing one, two, or four tandem synthetic fragments, respectively, are shown. Arrows indicate the 5′ → 3′ orientation of the T-rich strand of each consensus element. The numbers at the top (*Center* and *Right*) are the loss rate for the respective plasmid (9). HFT, high-frequency transformation. (Bar = 100 bp.)

tions using these parameters accurately reflect the helical stability and melting properties of DNA oligomers (25). The reliability and applicability of our helical stability calculation for high molecular weight DNA are demonstrated by the correct prediction, from all possible sites in the 6079-bp C2G1 plasmid, of both the location and hierarchy of nuclease-hypersensitive sites (Fig. 3).

We used the computer program to determine the helical stability of C2G1 *ARS* derivatives with mutations in the 3′-flanking sequence. Comparison of these data with the plasmid loss rates of the mutant C2G1 derivatives (9) provided a quantitative test for a relationship between helical instability of the 3′-flanking region and replication origin function. An important feature of our analysis in relation to deletion mutations is that the free energy calculation evaluates the consequences of not only the sequences removed but also the sequences brought into the 100-bp 3′-flanking region. The analysis of deletion derivatives reveals a quantitative association between the helical instability of an individual *ARS* mutant and its plasmid replication efficiency. This quantitative association indicates that the helical stability at the 3′-flanking region can alone account for the deleterious effects of mutations on the replication efficiency of the C2G1 *ARS*.

A role for helical instability of the 3′-flanking region in the function of the wild-type C2G1 *ARS* is entirely consistent with previous findings based on nuclease hypersensitivity of the H4 *ARS* and its mutant derivatives (12). We call the cis-acting sequence whose helical instability is required for replication origin function a DNA unwinding element (DUE) (15, 16). The DUE is an unusual genetic element in that its biological function is determined by the energetics of DNA unwinding and not a particular DNA sequence (refs. 15 and 16; this report). The DUE is dissimilar from other cis-acting elements, such as protein recognition sites, which are strictly conserved in DNA sequence, or spacer sequences, which are conserved in length, although the DUE may, in part, overlap with such elements (16).

A variety of DNA sequences may satisfy the energy requirements for unwinding the DUE at the origin since the primary sequence of the broad 3′-flanking region is not conserved among yeast *ARS* elements (6) and tolerates a variety of mutations (reviewed in ref. 34). In fact, a nuclease-hypersensitive sequence derived from pBR322 can functionally substitute for the H4 *ARS* 3′-flanking region (12). The DNA helix in this region of pBR322 is thermodynamically unstable as shown by two-dimensional gel electrophoresis of plasmid topoisomers (14) and by computer analysis (Fig. 3, thin arrow). Others have suggested that the functional substitution of the H4 *ARS* 3′-flanking region was mediated by specific sequences within the pBR322 fragment that are 9 of 11 matches to the consensus sequence and that may bind an initiator protein (9). However, it is now clear that such near-match sequences are not required for H4 *ARS* function since simultaneous point disruption of all near-match sequences within the 3′-flanking region, including 8 of 11 matches, does not affect plasmid replication efficiency (35). The simultaneous point mutations change the ΔG by <1 kcal/mol (unpublished results). In contrast, deletion mutations that remove near matches from the C2G1 *ARS* (9) lead to large increases in the free energy cost of unwinding (Figs. 4 and 5; derivatives with deletions beyond position 91). The effects of deletion mutations in the C2G1 *ARS* that implicated a role for multiple near-match sequences (9) can be accounted for by the contribution that such sequences make to the overall ease of unwinding the broad 3′-flanking region (Figs. 4 and 5). Consistent with this interpretation, tandem multimerization of the core consensus sequence creates a broad region of helical instability that accompanies increased replication efficiency (Fig. 6).

Our findings show that the requirement for a DNA unwinding element oriented 3′ to the essential consensus element, demonstrated only for the H4 *ARS* (12, 15), is conserved in the C2G1 *ARS*. Thus, the C2G1 *ARS*, a known chromosomal replication origin (cited in ref. 26), shares common components and a common organization with an *ARS* element that is only known to function as a plasmid replication origin. The ability to identify DUEs and quantitate their helical stabilities based on DNA sequence information should prove useful for the functional dissection of additional replication origins from yeast as well as those from other species.

We gratefully acknowledge the contributions of Robert Umek and William Whitford to the initial phase of these studies. We thank Martha Eddy for excellent technical assistance, and Joel Huberman, Charles Miller, and Ruea-Yea Huang for helpful comments on the manuscript. This research was supported by grants from the National Institutes of Health, General Medical Sciences.

1. Brewer, B. J. & Fangman, W. L. (1987) *Cell* **51**, 463–471.
2. Huberman, J. A., Spotila, L. D., Nawotka, K. A., El-Assouli, S. M. & Davis, L. R. (1987) *Cell* **51**, 473–481.
3. Huberman, J. A., Zhu, J., Davis, L. R. & Newlon, C. S. (1988) *Nucleic Acids Res.* **16**, 6373–6384.
4. Linskens, M. H. K. & Huberman, J. A. (1988) *Mol. Cell. Biol.* **8**, 4927–4935.
5. Stinchcomb, D. T., Struhl, K. & Davis, R. W. (1979) *Nature (London)* **282**, 39–43.
6. Broach, J. R., Li, Y.-Y., Feldman, J., Jayaram, M., Nasmyth, K. A. & Hicks, J. B. (1983) *Cold Spring Harbor Symp. Quant. Biol.* **47**, 1165–1173.
7. Celniker, S. E., Sweder, K., Srienc, F., Bailey, J. E. & Campbell, J. L. (1984) *Mol. Cell. Biol.* **4**, 2455–2466.
8. Bouton, A. H. & Smith, M. M. (1986) *Mol. Cell. Biol.* **6**, 2354–2363.
9. Palzkill, T. G. & Newlon, C. S. (1988) *Cell* **53**, 441–450.
10. Walker, S. S., Francesconi, S. C. & Eisenberg, S. (1990) *Proc. Natl. Acad. Sci. USA* **87**, 4665–4669.
11. Newlon, C. S. (1988) *Microbiol. Rev.* **52**, 568–601.
12. Umek, R. M. & Kowalski, D. (1988) *Cell* **52**, 559–567.
13. Umek, R. M. & Kowalski, D. (1987) *Nucleic Acids Res.* **15**, 4467–4480.
14. Kowalski, D., Natale, D. A. & Eddy, M. J. (1988) *Proc. Natl. Acad. Sci. USA* **85**, 9464–9468.
15. Umek, R. M. & Kowalski, D. (1990) *Proc. Natl. Acad. Sci. USA* **87**, 2486–2490.
16. Kowalski, D. & Eddy, M. J. (1989) *EMBO J.* **8**, 4335–4344.
17. Bramhill, D. & Kornberg, A. (1988) *Cell* **52**, 743–755.
18. Schnos, M., Zahn, K., Inman, R. B. & Blattner, F. R. (1988) *Cell* **52**, 385–395.
19. Borowiec, J. A., Dean, F. B., Bullock, P. A. & Hurwitz, J. (1990) *Cell* **60**, 181–184.
20. Gutierrez, C., Guo, Z.-S., Roberts, J. & DePamphilis, M. L. (1990) *Mol. Cell. Biol.* **10**, 1719–1728.
21. Caddle, M. S., Lussier, R. H. & Heintz, N. H. (1990) *J. Mol. Biol.* **211**, 19–33.
22. Linskens, M. H. K. & Huberman, J. A. (1990) *Cell* **62**, 845–847.
23. Felsenfeld, G. & Miles, H. T. (1967) *Annu. Rev. Biochem.* **36**, 407–448.
24. Wells, R. D., Larson, J. E., Grant, R. C., Shortle, B. E. & Cantor, C. R. (1970) *J. Mol. Biol.* **54**, 465–497.
25. Breslauer, K. J., Frank, R., Blöcker, H. & Marky, L. A. (1986) *Proc. Natl. Acad. Sci. USA* **83**, 3746–3750.
26. Van Houten, J. V. & Newlon, C. S. (1990) *Mol. Cell. Biol.* **10**, 3917–3925.
27. Palzkill, T. G., Oliver, S. G. & Newlon, C. S. (1986) *Nucleic Acids Res.* **14**, 6247–6264.
28. Holmes, D. S. & Quigley, M. (1981) *Anal. Biochem.* **114**, 193–197.
29. Radloff, R., Bauer, W. & Vinograd, J. (1967) *Proc. Natl. Acad. Sci. USA* **57**, 1514–1521.
30. Kowalski, D. & Sanford, J. P. (1982) *J. Biol. Chem.* **257**, 7820–7825.
31. Maxam, A. M. & Gilbert, W. (1980) *Methods Enzymol.* **65**, 499–560.
32. Sheflin, L. G. & Kowalski, D. (1984) *Nucleic Acids Res.* **12**, 7087–7104.
33. Marky, L. A. & Breslauer, K. J. (1987) *Biopolymers* **26**, 1601–1620.
34. Umek, R. M., Linskens, M. H. K., Kowalski, D. & Huberman, J. A. (1989) *Biochim. Biophys. Acta* **1007**, 1–14.
35. Holmes, S. G. & Smith, M. M. (1989) *Mol. Cell. Biol.* **9**, 5464–5472.